UDC 528.852.1 **doi: 10.32620/aktt.2023.1.07**

Galina PROSKURA, Oleksii RUBEL, Sergii KRYVENKO, Vladimir LUKIN

National Aerospace University "Kharkiv Aviation Institute", Kharkiv, Ukraine

ON CLASSIFIER PERFORMANCE FOR REMOTE SENSING IMAGES COMPRESSED BY DIFFERENT CODERS

Remote sensing data are widely used in numerous applications. A conventional task solved using remote sensing images is their classification. The classification maps are commonly produced by some pre-trained classifiers applied either to uncompressed or compressed images where lossy compression is often needed and employed in practice due to the necessity to reduce data volume at stages of image transfer and storage. Then, the classification accuracy depends on the characteristics of an image, a classifier, and a coder used. The main ***subject*** *of this paper is the factors that determine classification accuracy. One of them is compressed image quality. We fix the quality of compressed image quality characterized by the peak signal-to-noise ratio for several coders and rely on the same training approach. Our* ***goal*** *is twofold. First, we would like to consider classification accuracy for two approaches to classifier training: based on undistorted data and images with simulated distortions. Second, our desire is to compare the performance of different techniques of image compression. The* ***task*** *of this paper is to obtain an idea is it worth training the neural network classifier for uncompressed images or images of similar quality to the quality of compressed data to be classified. The coder's influence on classification results is of special interest as well. The main* ***results*** *are the following. First, the classification accuracy is almost the same for classifiers trained for uncompressed and simulated compressed data for the general distortion model. Second, there is a certain difference in the classification results for different compression techniques studied. Lightly better classification results are observed for data produced by more sophisticated (modern) coders. Experiments have been carried out for two real-life three-channel Sentinel-2 images of Kharkiv and the Kharkiv region having different complexity. Four typical classes have been considered. As a* ***conclusion****, it is possible to state that either the general model of distortions must be modified or the classifier training should be performed for data produced by the corresponding compression technique.*

Keywords: *lossy compression; three-channel images; neural network classifier; training data.*

Introduction

Remote sensing (RS) from spaceborne and airborne platforms has found a variety of important applications recently [1, 2]. A common intermediate or final task in RS data processing is image classification [3, 4]. Meanwhile, before classification, RS images are often processed where the processing might include different operations [5, 6]. Image compression is one of them [7-9]. The need for it arises due to the large volume of collected and processed RS data as well as the restricted bandwidth of communication lines and/or storage space. Whilst lossless compression does not introduce distortions, compression ratio (CR) reached for methods belonging to this group often occurs to be inappropriate for practice [10, 11]. In turn, lossy compression techniques are able to provide a considerably larger and variable CR [12-14]. However, distortions introduced by lossy compression affect classification in a specific way [9, 14, 15]. In some cases, even improvement of classification accuracy is possible [14]. Meanwhile, in most cases, the probability of correct classification tends to decrease if the compression ratio increases and, hence, the introduced distortions become larger [15, 16].

In general, classification accuracy depends on several factors, namely, the classifier used [9], its training strategy [16], compression ratio attained, employed coder, image complexity [15, 16], etc. Here, we consider the neural network (NN) based approach [17] to classification that has been earlier used in our papers [15, 16]. The reason for this is that NN-based approaches are powerful and often used for RS data classification [18] due to their ability to incorporate non-Gaussian properties of features exploited. The NN-classifier performance also depends on image complexity, the number of classes and their separability, training sample size, and methodology of learning. In particular, in [16], it has been shown the following. If the classifier has been trained for undistorted data and then applied to compressed images, then the probability of correct classification has the tendency to reduce with CR increasing, especially for complex structure images containing a lot of textures, edges, and small-sized details (objects). On the other hand, the probability of correct classification for compressed images can be slightly increased if the classifier training has been carried out for images with a similar level of distortions. Note that distortions due to lossy compression in [16] have been modelled as additive white Gaussian

noise based on preliminary analysis of statistical and spatial spectral characteristics of distortions [15] for several coders. However, characteristics and specific features of distortions are individual for different image compression methods. The most known peculiarities are the blocking artifacts for JPEG [19] and Gibbs phenomenon for JPEG2000 and SPIHT [20]. The model in [15] takes into account only the facts that distortions due to lossy compression have quasi-Gaussian distribution and are practically spatially correlated. These distortions are easy to simulate to model the desired peak signal-to-noise ratio (PSNR) of distorted images.

Keeping this in mind, our **idea** is to produce images having the same PSNR for different coders and to analyze the characteristics of their compression and classification. Such a study should give answers to different questions the main of which are the following: 1) is it worth using uncompressed or generally simulated images for NN training?; 2) do different coders produce approximately the same or sufficiently different results for the same PSNR of compressed images?

Problem statement

Since compression artifacts and classification results usually depend on image complexity, it is reasonable to perform our studies for, at least, two images of different complexity. Thus, **we** have chosen the images SS1 and SS2 composed of visual range components of Sentinel-2 multispectral data and visualized as RGB color images (Fig. 1). As one can see, the image in Fig. 1,a has a simpler structure than the image in Fig. 1,b since the former image corresponds to the countryside region (Stariy Saltiv, Kharkiv Region) whilst the latter image relates to the North part of Kharkiv with neighbor forests and agricultural fields.

We have used four coders. The first and second ones called AGU and ADCT, respectively, are based on discrete cosine transform where AGU [21] employs fixed 32x32 pixel block size and the ADCT [22] coder uses an optimized partition scheme for adapting the block size to image local content. JPEG2000 is the known standard [20] whilst the fourth analyzed coder called better portable graphics (BPG) [23, 24] is known to be a part of the video compression standard HEVC [25]. Thus, the coders are based on different orthogonal transforms (DCT and wavelets) and exploit different parameters that control compression (PCC) – quantization step (QS) for the AGU and ADCT coders, bits per pixel (BPP) for JPEG2000, and the parameter Q (which is an integer from 1 to 51) for the BPG encoder. All coders allow providing a desired PSNR quite accurately for a fair comparison of the obtained results.

Thus, our task consists in determining whether is it reasonable to use the distortion-free or general model-based distorted image for NN classifier training. Another task is to compare the classifier performance for compressed images having identical quality (according to the PSNR criterion) but compressed by different coders. Note that we consider the case of PSNR=31 dB, i.e. mean square error of introduced distortions about 50 (for three-channel images with the 8-bit representation of data for each component.

a

b

Fig. 1. The considered real-life three-channel images of the country-side (a) and urban (b) areas

Table 1 gives data that allow getting some preliminary imagination concerning the coder performance for both images. From the very beginning, let us explain why we have decided to consider setting the desired PSNR equal to 31 dB. First, such a value was used (as one of four possible) in the papers [15, 16]. Second,

PSNR=31 dB corresponds to the case when the introduced distortions are visible for practically all images irrespective of their complexity. Third, it has been found earlier that the probability of correct classification starts to radically reduce when distortions become visible.

Table 1

Performance characteristics of coders for two considered images

Image	Coder	CR			PSNR		
		R	G	B	R	G	B
SS1	AGU	39.8	36.0	57.4	31.0	30.9	31.0
SS1	ADCT	45.1	38.4	62.9	31.0	31.0	30.9
SS1	BPG	50.4	44.7	70.1	31.0	30.8	31.1
SS1	JPEG2000	32.0	27.1	44.7	30.9	31.1	31.0
SS2	AGU	5.23	5.22	5.3	31.1	30.9	31.0
SS2	ADCT	5.68	5.42	5.76	31.0	31.1	30.9
SS2	BPG	6.44	6.30	6.47	30.8	30.7	30.7
SS2	JPEG2000	5.02	5.00	5.01	31.2	30.9	31.1

a

b

Fig. 2. Image SS1 compressed by AGU (a) and JPEG2000 (b)

The examples given in Fig. 2 show that the introduced distortions are visible (both images are smeared) compared to the original image in Fig. 1,a. Although for both images PSNR is equal to 31 dB, the difference in them can be found by attentive observation.

Data in Table 2 show that the desired PSNR has been provided quite accurately for all coders for both images (the worst accuracy takes place for the BPG coder for which PCC Q can fall only to integers). All coders have been applied component-wise. For image SS1, the compression ratio for the "blue" component is larger than for the other two components. For image SS2, the CR values are approximately the same for all three components (for each coder). Meanwhile, the CR values for the simpler structure image (SS1) are by many times larger than for the complex structure image (SS2). The ADCT and, especially, BPG coders provide sufficiently larger CR than AGU and, especially, JPEG2000. Thus, for the same quality (characterized by PSNR), BPG and ADCT coders have certain advantages. However, here we are more interested in indicators of classification accuracy discussed in the next Section than in CR.

Analysis of classification accuracy

Before starting the analysis of the obtained data, let us remind a few details about the classifier used. First, we dealt with multichannel images acquired by the Sentinel-2 satellite sensor at the end of August 2019. Four visually distinguishable classes have been studied: 1 – Urban, 2 – Water, 3 – Vegetation, and 4 – Bare Soil for which the features intersect considerably.

Since we had the maps of the corresponding territories sensed, homogeneous fragments of images that represent the aforementioned classes have been marked by experts. They have been marked with a conditional color corresponding to each class as follows: Urban - yellow, Water - blue, Vegetation - green, Bare Soil - black. The sets of the marked pixels have been divided into two subsets: the training and control (verification) samples (Fig. 3 and 4).

The sizes of the training samples were from 4×10^3 to 20×10^3 pixels, and the sizes of the verification samples were larger – from 7×10^3 to 50×10^3 pixels. Thus, the classes were representative enough.

Only the three pixel (voxel) values have been used as input features. In other words, we have not used any textural information (that, in general, could be helpful for better classification). The classification information from neighbor pixels has not been aggregated (although this could improve classification as well). Therefore, a simple pixel-wise classification approach has been employed to understand and compare the classifier performance for different coders with any "assistance" of post-classification techniques.

ISSN 1814-4225 (print)
ISSN 2663-2012 (online)

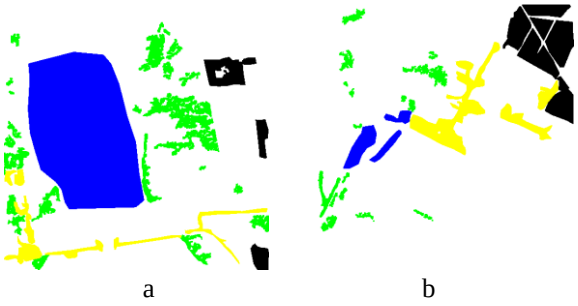

a b

Fig. 3. Fragments used for the classifier training for images SS1 (a) and SS2 (b)

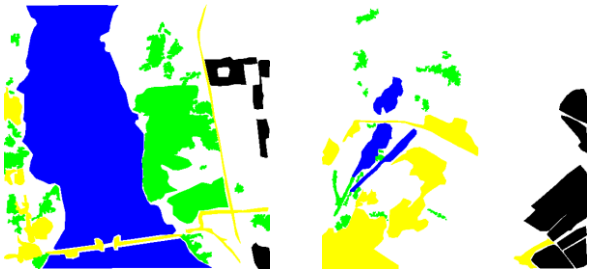

a b

Fig. 4. Fragments used for the classifier verification for images SS1 (a) and SS2 (b)

Although we have already decided that the classifier to be used is based on an NN, there is a wide space of options for what NN and with what parameters to choose. Since we have only three input parameters (features), a small number of classes (four), and a limited sample size (thousands) for NN training, we have decided to use a simple NN - a multilayer perceptron (MLP) with supervised learning based on backpropagation. It has an input layer, an output layer, and several hidden layers. With the exception of input neurons, all other neurons commonly use a non-linear activation function. In our case, the NN has 4 hidden layers containing 64, 32, 16 and 8 neurons respectively.

The optimal parameters of MLP (the number of hidden layers, neurons in them, and the learning function) have been determined by experiments with a single data set. The ReLU (Rectified Linear Unit) activation function has been used in hidden layers. The linear activation function has been used for the output layer. The RMSProp optimizer has been employed in MLP training. Cross-entropy has been used as a loss function. More details concerning the MLP and its training can be found in [16].

Classification accuracy can be characterized in different ways including confusion matrices, probabilities of correct classification for particular classes and in aggregate, as well as by F1-measure as an efficiency estimation metric [12, 26]. The latter indicator (criterion) is a harmonic mean of accuracy and completeness (accuracy indicates how many of the objects identified by the classifier as positive are indeed positive; completeness shows how many of the positive objects have been identified by the classifier). An important property of the harmonic mean is that it approaches zero if, at least, one of these arguments approaches zero. In the multi-class case, F-measure is determined as the average of the F1-measures of each class with the corresponding weighting [12].

Let us start with the image SS1 where the MLP has been trained for the uncompressed image. The obtained data are presented in Table 2. Analysis shows that the class Water is recognized very well, the class Vegetation is recognized well, and the classes Bare Soil and Urban are recognized not well because of a high percentage of misclassifications between them. Although there are certain variations of F1 values for particular classes for different coders, the total values are very close.

If the classifier has been trained for the simulated (noisy, PSNR=31 dB) compressed image, the situation changes – the corresponding data are presented in Table 3. F1 values decrease for two classes for the coder JPEG2000 and for all classes for three other coders. As a result, the total (aggregate) F1 values have decreased as well: by about 0.02 for the coders ADCTm AGU, and BPG, and by about 0.01 for JPEG2000 where the results for the coder JPEG2000 occurred to be the best where the worst results have been observed for data compressed by the AGU coder.

Table 2

Classification data (F1-measures) for image SS1 with MLP training for uncompressed image

Class	Coder			
	ADCT	AGU	BPG	JPEG2000
Urban	0.78	0.81	0.81	0.81
Water	0.99	0.99	0.99	0.99
Vegetation	0.95	0.94	0.94	0.94
Bare soil	0.76	0.76	0.75	0.76
Total	0.9526	0.9533	0.9527	0.9543

Table 3

Classification data (F1-measures) for image SS1 with MLP training for simulated compressed image

Class	Coder			
	ADCT	AGU	BPG	JPEG2000
Urban	0.71	0.77	0.72	0.83
Water	0.98	0.98	0.98	0.98
Vegetation	0.91	0.91	0.92	0.92
Bare soil	0.72	0.74	0.72	0.77
Total	0.9301	0.9347	0.9353	0.9457

Thus, for image SS1, it has happened that it is worth using the MLP training for uncompressed image. The classification results obtained for MLP training for the simulated "general" compressed image are not too much but worse.

Fig. 5 represents the classification maps obtained for the classifier trained for the general simulated image applied to the data at the output of the considered coders. The classification results are quite similar although differences can be easily found. As one can see, there are many pixels misclassified from the class Vegetation to the class Water. There are also misclassifications between the classes Urban and Bare Soil.

Let us now consider the data obtained for image SS2. Consider the case when the MLP has been trained for the uncompressed image. The data obtained are given in Table 4. This time the classes Urban and Bare Soil are recognized well whilst the classes Vegetation and Water are recognized badly because of a lot of misclassifications between them. There are variations of F1 values for particular classes for different coders, but the total values are quite close. The best results this time are obtained for the image compressed by BPG whilst the smallest F1 values are again observed for the image compressed by AGU.

Assume now that the classifier has been trained for the simulated compressed image (see data in Table 5). F1 values have decreased (compared to the corresponding data in Table 4) for the class Bare Soil for all coders but radically improved for the class Water. For other classes, small changes take the place. As a result, the total (aggregate) F1 values practically have not changed except for the data for the AGU coder for which the F1 increase by about 0.01 has taken place.

The results are still the best for the BPG coder and the worst for the image compressed by the AGU coder. As one can see, for the complex structure image, it almost does not matter what image to use for the MLP training.

Fig. 6 presents the classification maps for the classifier trained for the uncompressed image SS2 applied to the data for all four considered coders. The classification results are again very similar although it is again possible to find the differences. There are many pixels misclassified between the classes Vegetation and the class Water.

Table 4

Classification data (F1-measures) for image SS2 with MLP training for uncompressed image

Class	Coder			
	ADCT	AGU	BPG	JPEG2000
Urban	0.91	0.90	0.91	0.90
Water	0.71	0.69	0.70	0.72
Vegetation	0.63	0.59	0.64	0.64
Bare soil	0.89	0.88	0.90	0.89
Total	0.8461	0.8275	0.8521	0.8431

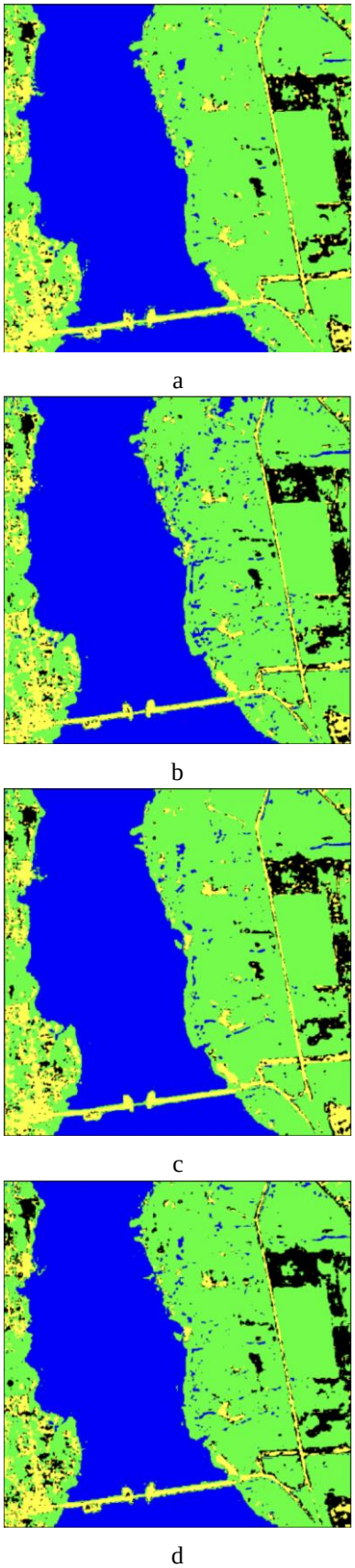

a

b

c

d

Fig. 5. Classification maps for images compressed by the coders ADCT (a), AGU (b), BPG (c), and JPEG2000 obtained by the MLP-classifier trained for the general simulated compressed image

ISSN 1814-4225 (print)
ISSN 2663-2012 (online)

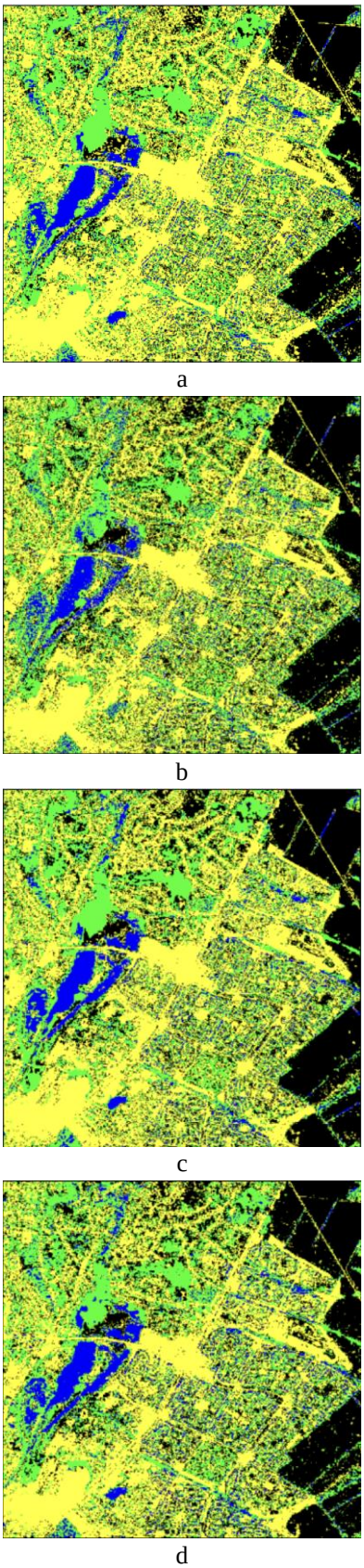

a

b

c

d

Fig. 6. Classification maps for images compressed by the coders ADCT (a), AGU (b), BPG (c), and JPEG2000 (d) obtained by the MLP-classifier trained for the uncompressed image

Table 5

Classification data (F1-measures) for image SS2 with MLP training for simulated compressed image

Class	Coder			
	ADCT	AGU	BPG	JPEG2000
Urban	0.91	0.90	0.89	0.90
Water	0.75	0.79	0.84	0.75
Vegetation	0.60	0.59	0.69	0.64
Bare soil	0.88	0.86	0.87	0.88
Total	0.8463	0.8375	0.8517	0.8408

There are fewer misclassifications between the classes Urban and Bare Soil (compared to image SS1). Since many areas correspond to private houses with gardens, we have a lot of mixed pixels and "mosaic" results of classification.

Finally, let us give two examples of classification maps for the MLP classifier trained for the noisy image (Fig. 7). One specific feature of these two maps is that many pixels have been classified as Water (in the right part of both images) although they correspond to the classes Urban or Vegetation (in fact, these are typical city regions with multi-store buildings and trees around them). The possible reason is that, by adding noise to the image to be used for training, we "expand" the features that correspond to the class Water and make them intersect more with feature spaces for other classes.

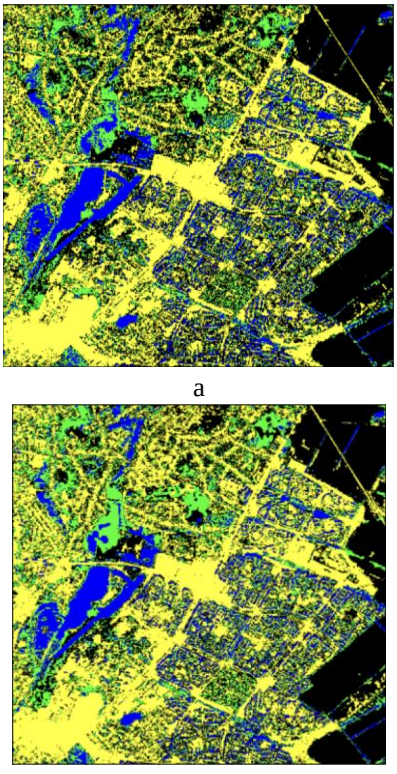

a

b

Fig. 7. Classification maps for images compressed by the coders BPG (a), and JPEG2000 (b) obtained by the MLP-classifier trained for the simulated image

Thus, we can put forward two hypotheses. First, the AWGN model of distortions introduced by lossy compression is not adequate enough (is too simple or is not valid for all lossy compression techniques or all images or all compression ratios). Second, particular coders might introduce specific distortions that are worth taking into account at the classifier training stage. Putting aside the former hypothesis, let us check the latter one.

Classification with adaptation to properties of particular coders

Thus, let us see what are the classification results if the classifier is trained for fragments of the image compressed by a given coder and then applied to other fragments of this image. The F1 values for image SS1 are presented in Table 6. Comparing these data to the corresponding data in Tables 2 and 3, it is possible to see that the total probabilities are larger than both total probabilities for other ways of the classifier training. Note that the total probabilities for data produced by different coders are very close.

Table 6

Classification data (F1-measures) for image SS1 with MLP training for the same compressed image

Class	Coder			
	ADCT	AGU	BPG	JPEG2000
Urban	0.83	0.83	0.83	0.82
Water	1.0	0.99	1.00	0.99
Vegetation	0.96	0.95	0.95	0.95
Bare soil	0.77	0.77	0.75	0.78
Total	0.9622	0.9578	0.9589	0.9583

Table 7 gives data for the same training methodology but for the image SS2. The obtained results can be compared to the corresponding results in Tables 4 and 5. As one can see, the values of F1 have improved (increased) compared to the corresponding values in Tables 4 and 5. The best classification results are reached for data produced by the BPG coder.

Table 7

Classification data (F1-measures) for image SS2 with MLP training for the same compressed image

Class	Coder			
	ADCT	AGU	BPG	JPEG2000
Urban	0.91	0.91	0.92	0.91
Water	0.77	0.77	0.74	0.74
Vegetation	0.65	0.60	0.66	0.65
Bare soil	0.87	0.89	0.89	0.89
Total	0.8480	0.8405	0.8546	0.8482

Hence, we can conclude that if one plans to classify compressed images, it is worth using for training the data compressed by the same coder (and with similar quality characterized by PSNR).

Fig. 8 presents two classification maps for images compressed by the coders BPG and JPEG2000 obtained by the MLP classifier trained for the corresponding compressed images. As one can see, the classification maps in Fig. 8 are very similar to each other. Compared to the maps in Fig. 7, there are fewer misclassifications to the class Water in the urban region in the right part of the image.

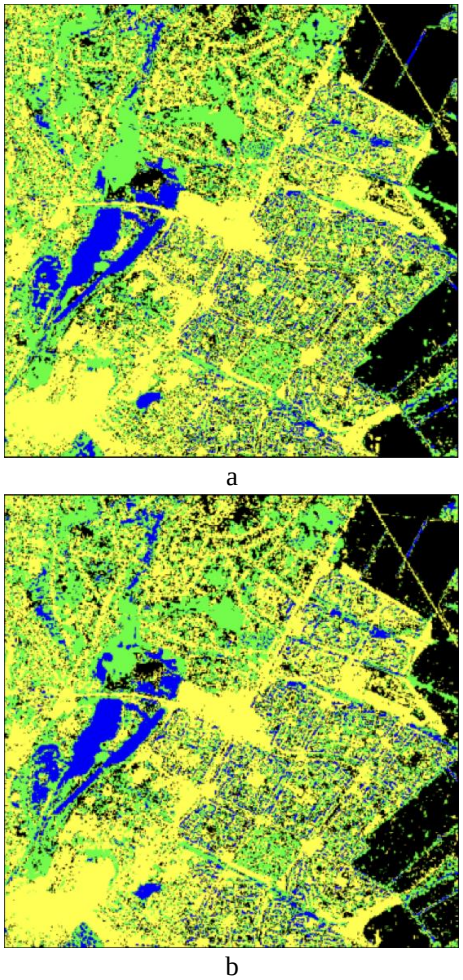

a

b

Fig. 8. Classification maps for images compressed by the coders BPG (a), and JPEG2000 (b) obtained by the MLP-classifier trained for the same compressed images

Conclusions

The presented results obtained for two images of natural scenes of different complexity show that, if compressed images are planned to be classified, it is reasonable to carry out the classifier training for compressed data but only under the condition that the data used for

training have been obtained for the same coder and with similar characteristics of compression. The use of the general model of simulated compressed data for training is not so efficient. There are two possible reasons behind this. First, the current version of the general model is too simplified. Second, it does not take into account the peculiarities of particular coders.

Contributions of authors: conceptualization – **Vladimir Lukin, Galina Proskura;** methodology – **Sergii Kryvenko, Vladimir Lukin;** formulation of tasks **– Galina Proskura, Oleksii Rubel;** analysis **– Galina Proskura, Vladimir Lukin;** development of model **– Sergii Kryvenko, Oleksii Rubel;** software **– Oleksii Rubel, Sergii Kryvenko;** verification **– Galina Proskura, Vladimir Lukin;** analysis of results **– Vladimir Lukin, Galina Proskura;** visualization **– Galina Proskura;** writing – original draft preparation **– Galina Proskura;** writing – review and editing **– Vladimir Lukin.**

All the authors have read and agreed to the published version of the manuscript.

References (GOST 7.1:2006)

1. Crop inventory at regional scale in Ukraine: Developing in season and end of season crop maps with multi-temporal optical and SAR satellite imagery [Text] / N. Kussul, M. Lavreniuk, A. Shelestov, S. Skakun // European Journal of Remote Sensing. – 2018. – Vol. 51, iss. 1. – P. 627-636. DOI: 10.1080/22797254.2018.1454265.

2. Potential Applications of the Sentinel-2 Multispectral Sensor and the ENMAP hyperspectral Sensor in Mineral Exploration [Text] / C. Mielke, N. K. Boshce, C. Rogass, K. Segl, C. Gauert, H. Kaufmann // EARSeL eProceedings. – 2014. – Vol. 13, Iss. 2. – P. 93-10, DOI: 10.12760/01-2014-2-07.

3. Sisodia, P. S. Analysis of Supervised Maximum Likelihood Classification for remote sensing image. [Text] / P. S. Sisodia, V. Tiwari, A. Kumar // International Conference on Recent Advances and Innovations in Engineering (ICRAIE-2014). – 2014. – P. 1-4. DOI: 10.1109/ICRAIE.2014.6909319.

4. Parcel-Based Crop Classification in Ukraine Using Landsat-8 Data and Sentinel-1A Data [Text] / N. Kussul, G. Lemoine, F. J. Gallego, S. Skakun, M. Lavreniuk, A. Shelestov // IEEE Journal of Selected Topics in Applied Earth Observations and Remote Sensing. – 2016. – No. 9. – P. 2500-2508. DOI: 10.1109/JSTARS.2016.2560141.

5. Zhong, P. Multiple-Spectral-Band CRFs for Denoising Junk Bands of Hyperspectral Imagery [Text] / P. Zhong, R. Wang // IEEE Transactions on Geoscience and Remote Sensing. – 2013. – Vol. 51, iss. 4. – P. 2269-2275. DOI: 10.1109/TGRS.2012.2209656.

6. Hyperspectral Remote Sensing Data Analysis and Future Challenges [Text] / J. M. Bioucas-Dias, A. Plaza, G. Camps-Valls, P. Scheunders, N. Nasrabadi, J. Chanussot // IEEE Geoscience and Remote Sensing Magazine. – 2013. – Vol. 1. – P. 6-36. DOI: 10.1109/MGRS.2013.2244672.

7. Spectral distortion in lossy compression of hyperspectral data [Text]/ B. Aiazzi, L. Alparone, S. Baronti et al. // Journal of Electrical Computer Engineering. – 2012. – Vol. 2012. DOI: 10.1155/2012/850637.

8. Oh, H. Visually lossless JPEG 2000 for remote image browsing [Text] / H. Oh, A. Bilgin, M. Marcellin // Information. – 2016. – Vol. 7, iss. 3. – Article No. 45. DOI: 10.3390/info7030045.

9. Effects of JPEG and JPEG2000 lossy compression on remote sensing image classification for mapping crops and forest areas [Text] / A. Zabala, X. Pons, R. Díaz-Delgado et al. // Proceding of 2006 IEEE International Symposium on Geoscience and Remote Sensing. – 2006. – P. 790-793. DOI: 10.1109/IGARSS.2006.203.

10. Hussain, A. J. Image compression techniques: A survey in lossless and lossy algorithms [Text] / A. J. Hussain, A. Al-Fayadh, N. Radi // Neurocomputing. – 2018. – Vol. 300. – P. 44-69. DOI: 10.1016/j.neucom.2018.02.094.

11. Sayood, K. Introduction to data compression [Text] / K. Sayood. – San Francisco : Morgan Kaufmann, 2017. – 680 p.

12. Deep learning-based picture-wise just noticeable distortion prediction model for image compression [Text] / H. Liu, Y. Zhang, H. Zhang et al. // IEEE Transactions on Image Processing. – 2019. – Vol. 29. – P. 641-656. DOI: 10.1109/TIP.2019.2933743.

13. Li, F. Two-step providing of desired quality in lossy image compression by SPIHT [Text] / F. Li, S. Krivenko, V. Lukin // Radioelectronic and computer systems. – 2020. – No. 2. – P. 22-32. DOI: 10.32620/reks.2020.2.02.

14. Ozah, N. Compression improves image classification accuracy [Text]/ N. Ozah, A. Kolokolova // Proceedings of Canadian Conference on Artificial Intelligence. – 2019. – P. 525-530. DOI: 10.1007/978-3-030-18305-9_55.

15. Image Classification Accuracy Analysis for Three-channel Remote Sensing Data [Text] / F. Li, V. Lukin, G. Proskura, I. Vasilyeva, G. Chernova // Proceedings of the conference "Intelligent Information technologies and systems of information security" IntelITSIS-2022, Ukraine, 2022. – 15 p.

16. Proskura, G. On classifier learning methodologies with application to compressed remote sensing images. [Text] / G. Proskura, V. Lukin, O. Rubel // Radioelectronic and computer systems. – 2022. – No. 3. – P. 174-189. DOI: 10.32620/reks.2022.3.13.

17. Bishop, Ch. M. Pattern Recognition and Machine Learning [Text] / Ch. M. Bishop. – Springer, 2010. – 738 p.

18. Ustuner, M. Comparison of Neural Network and ISODATA classifiers for Land Cover Assessment Using Optical Data [Text] / M. Ustuner, F. B. Sanli // FIG Commission 3 Workshop 2012 Spatial Information, Informal Development, Property and Housing, 2012.

– P. 1-7. – Available at: https://www.researchgate.net/publication/259864255_Comparison_of_Neural_Network_and_ISODATA_classifiers_for_Land_Cover_Assessment_Using_Optical_Data. – 12.12.2022.

19. Pennebaker, W. B. JPEG-still Image Data Compression Standard [Text] / W. B. Pennebaker, J. L. Mitchel, Eds. – New York : Van Nostrand Reinhold, 1992. – 650 p.

20. Said, A. A new fast and efficient image codec based on the partitioning in hierarchical trees [Text] / A. Said, W. Pearlman // IEEE Trans. on Circuits Syst. Video Technology. – 1996. – Vol. 6. – P. 243-250. DOI 10.1109/76.499834.

21. DCT Based High Quality Image Compression [Text] / N. N. Ponomarenko, V. V. Lukin, K. Egiazarian, J. Astola // Proceedings of 14th Scandinavian Conference on Image Analysis. – Joensuu, Finland, June, 2005. – P. 1177-1185. DOI: 10.1007/11499145_119.

22. ADCTC: advanced DCT-based coder [Text] / N. Ponomarenko, V. Lukin, K. Egiazarian, J. Astola // Proceedings of the 2008 International Workshop on Local and Non-Local Approximation in Image Processing. – LNLA2008. – Switzerland, August 2008. – 6 p. – Available at: https://www.eurasip.org/Proceedings/Ext/LNLA2008/papers/cr1017.pdf. – 12.12.2022.

23. Albalawi, U. A hardware architecture for better portable graphics (BPG) compression encoder [Text] / U. Albalawi, S. P. Mohanty, E. Kougianos // Proceedings of 2015 IEEE International Symposium on Nanoelectronic and Information Systems. – 2015. – P. 291-296, DOI: 10.1109/iNIS.2015.12.

24. Medical image compression based on region of interest using better portable graphics (BPG) [Text] / D. Yee, S. Soltaninejad, D. Hazarika, G. Mbuyi, R. Barnwal, A. Basu // 2017 IEEE International Conference on Systems, Man, and Cybernetics (SMC). – 2017. – P. 216-221. DOI: 10.1109/SMC.2017.8122605.

25. Siqueira, I. Rate-Distortion and Complexity Comparison of HEVC and VVC Video Encoders [Text] / I. Siqueira, G. Correa, M. Grellert // 2020 IEEE 11th Latin American Symposium on Circuits & Systems (LASCAS). – San Jose, Costa Rica, 2020. – P. 1-4. DOI: 10.1109/LASCAS45839.2020.9069036.

26. Congalton, R. G. Assessing the Accuracy of Remotely Sensed Data: Principles and Practices [Text] / R. G. Congalton, K. Green. – Florida, USA : CRC Press, 1999. – 348 p.

References (BSI)

1. Kussul, N., Lavreniuk, M., Shelestov, A., Skakun, S. Crop inventory at regional scale in Ukraine: Developing in season and end of season crop maps with multi-temporal optical and SAR satellite imagery. *European Journal of Remote Sensing*, 2018, vol. 51, iss. 1, pp. 627-636. DOI: 10.1080/22797254.2018.1454265.

2. Mielke, C., Boshce, N. K., Rogass, C., Segl, K., Gauert, C., Kaufmann, H. Potential Applications of the Sentinel-2 Multispectral Sensor and the ENMAP hyperspectral Sensor in Mineral Exploration. *EARSeL eProceedings*, 2014, no. 13, iss. 2, pp. 93-10. DOI: 10.12760/01-2014-2-07.

3. Sisodia, P. S., Tiwari, V., Kumar, A. Analysis of Supervised Maximum Likelihood Classification for remote sensing image. *International Conference on Recent Advances and Innovations in Engineering (ICRAIE-2014)*, 2014, pp. 1-4. DOI: 10.1109/ICRAIE.2014.6909319.

4. Kussul, N., Lemoine, G., Gallego, F. J., Skakun, S., Lavreniuk, M., Shelestov, A. Parcel-Based Crop Classification in Ukraine Using Landsat-8 Data and Sentinel-1A Data. *IEEE Journal of Selected Topics in Applied Earth Observations and Remote Sensing*, 2016, no. 9, pp. 2500-2508. DOI: 10.1109/JSTARS.2016.2560141.

5. Zhong, P., Wang, R. Multiple-Spectral-Band CRFs for Denoising Junk Bands of Hyperspectral Imagery. *IEEE Transactions on Geoscience and Remote Sensing*, 2013, no. 51, iss. 4, pp. 2269-2275. DOI: 10.1109/TGRS.2012.2209656.

6. Bioucas-Dias, J. M., Plaza, A., Camps-Valls, G., Scheunders, P., Nasrabadi, N., Chanussot, J. Hyperspectral Remote Sensing Data Analysis and Future Challenges. *IEEE Geoscience and Remote Sensing Magazine*, 2013, vol. 1, pp. 6-36. DOI: 10.1109/MGRS.2013.2244672.

7. Aiazzi, B., Alparone, L., Baronti, S. et al. Spectral distortion in lossy compression of hyperspectral data. *Journal of Electrical Computer Engineering*, 2012, vol. 2012. DOI: 10.1155/2012/850637.

8. Oh, H., Bilgin, A., Marcellin, M. Visually lossless JPEG 2000 for remote image browsing. *Information*, 2016, vol. 7, iss. 3, article no. 45. DOI: 10.3390/info7030045.

9. Zabala, A., Pons, X., Díaz-Delgado, R. et al. Effects of JPEG and JPEG2000 lossy compression on remote sensing image classification for mapping crops and forest areas. *Proceedings of 2006 IEEE International Symposium on Geoscience and Remote Sensing*, 2006, pp. 790-793, DOI: 10.1109/IGARSS.2006.203.

10. Hussain, A. J., Al-Fayadh, A., Radi, N. Image compression techniques: A survey in lossless and lossy algorithms. *Neurocomputing*, 2018, vol. 300, pp. 44-69, DOI: 10.1016/j.neucom.2018.02.094.

11. Sayood, K. *Introduction to data compression*. San Francisco, Morgan Kaufmann Publ., 2017. 680 p.

12. Liu, H., Zhang, Y., Zhang, H. et al. Deep learning-based picture-wise just noticeable distortion prediction model for image compression. *IEEE Transactions on Image Processing*, 2019, vol. 29, pp. 641-656, DOI: 10.1109/TIP.2019.2933743.

13. Li, F., Krivenko, S., Lukin, V. Two-step providing of desired quality in lossy image compression by

SPIHT. *Radioelectronic and computer systems*, 2020, no. 2, pp. 22-32. DOI: 10.32620/reks.2020.2.02.

14. Ozah, N., Kolokolova, A. Compression improves image classification accuracy. *Proceedings of Canadian Conference on Artificial Intelligence*, 2019, pp. 525-530. DOI: 10.1007/978-3-030-18305-9_55.

15. Li, F., Lukin, V., Proskura, G., Vasilyeva, I., Chernova, G. Image Classification Accuracy Analysis for Three-channel Remote Sensing Data. *Proceedings of the conference "Intelligent Information technologies and systems of information security" IntelITSIS-2022, Ukraine, 2022.* 15 p.

16. Proskura, G., Lukin, V., Rubel, O. On classifier learning methodologies with application to compressed remote sensing images. *Radioelectronic and computer systems*, 2022, no. 3, pp. 174-189. DOI 10.32620/reks. 2022.3.13.

17. Bishop, Ch. M. *Pattern Recognition and Machine Learning*. Springer Publ., 2010. 738 p.

18. Ustuner, M., Sanli, F. B. Comparison of Neural Network and ISODATA classifiers for Land Cover Assessment Using Optical Data. *FIG Commission 3 Workshop 2012 Spatial Information, Informal Development, Property and Housing, 2012*, pp. 1-7. Available at: https://www.researchgate.net/publication/ 259864255_Comparison_of_Neural_Network_and_ ISODATA_classifiers_for_Land_Cover_Assessment_Using_Optical_Data (accessed 12.12.2022.)

19. Pennebaker, W. B., Mitchel, J. L. Eds. *JPEG-still Image Data Compression Standard*. New York, Van Nostrand Reinhold, 1992. 650 p.

20. Said, A., Pearlman, W. A new fast and efficient image codec based on the partitioning in hierarchical trees. *IEEE Trans. on Circuits Syst. Video Technology*, 1996, vol. 6, pp. 243-250. DOI: 10.1109/76.499834.

21. Ponomarenko, N. N., Lukin, V. V., Egiazarian, K., Astola, J. DCT Based High Quality Image Compression. *Proceedings of 14th Scandinavian Conference on Image Analysis*, Joensuu, Finland, June 2005, pp. 1177-1185. DOI: 10.1007/11499145_119.

22. Ponomarenko, N., Lukin, V., Egiazarian, K., Astola, J. ADCTC: advanced DCT-based coder. *Proceedings of the 2008 International Workshop on Local and Non-Local Approximation in Image Processing, LNLA2008*, Switzerland, August 2008. 6 p. Available at: https://www.eurasip.org/Proceedings/Ext/LNLA2008/ papers/cr1017.pdf. (accessed 12.12.2022.)

23. Albalawi, U., Mohanty, S. P., Kougianos, E. A hardware architecture for better portable graphics (BPG) compression encoder. *Proceedings of 2015 IEEE International Symposium on Nanoelectronic and Information Systems*, 2015, pp. 291-296. DOI: 10.1109/ iNIS.2015.12.

24. Yee, D., Soltaninejad, S., Hazarika, D., Mbuyi, G., Barnwal, R., Basu, A. Medical image compression based on region of interest using better portable graphics (BPG). *Proceedings of 2017 IEEE International Conference on Systems, Man, and Cybernetics (SMC)*, 2017, pp. 216-221. DOI: 10.1109/SMC.2017.8122605.

25. Siqueira, I., Correa, G., Grellert, M., Rate-Distortion and Complexity Comparison of HEVC and VVC Video Encoders. *Proceedings of the 2020 IEEE 11th Latin American Symposium on Circuits & Systems*, San Jose, Costa Rica, 2020, pp. 1-4. DOI: 10.1109/ LASCAS45839.2020.9069036.

26. Congalton, R. G., Green, K. Assessing the Accuracy of Remotely Sensed Data: Principles and Practices. Florida, USA, CRC Press Publ., 1999. 348 p.

Поступила до редакції 05.01.2023, прийнята до опублікування 20.02.2023

ЩОДО ХАРАКТЕРИСТИК РОБОТИ КЛАСИФІКАТОРА ДЛЯ ЗОБРАЖЕНЬ ДИСТАНЦІЙНОГО ЗОНДУВАННЯ, ЯКІ СТИСНУТІ РІЗНИМИ КОДЕРАМИ

Г. А. Проскура, О. С. Рубель, С. С. Кривенко, В. В. Лукін

Традиційним завданням, що вирішується за допомогою зображень ДЗЗ, є їх класифікація. Карти класифікації зазвичай створюються деякими попередньо навченими класифікаторами, які застосовуються до нестиснутих або стиснутих зображень, де часто потрібне стиснення з втратами, яке використовується на практиці через необхідність зменшити обсяг даних на етапах передачі та зберігання зображень. Тоді точність класифікації залежить від характеристик зображення, класифікатора та кодера, що використовується. Основним предметом статті є фактори, що визначають точність класифікації. Одним з них є якість стисненого зображення. Ми фіксуємо якість стисненого зображення, що характеризується піковим відношенням сигнал/шум для кількох кодерів і покладаємося на той самий підхід до навчання. Наша мета двояка. По-перше, ми хотіли б розглянути точність класифікації для двох підходів до навчання класифікаторів: на основі неспотворених даних і зображень із змодельованими спотвореннями. По-друге, ми хочемо порівняти ефективність різних технік стиснення зображення. Завдання цієї статті полягає в тому, щоб отримати уявлення про те, чи варто тренувати

класифікатор нейронної мережі для нестиснутих зображень або зображень із якістю, подібною до якості стиснутих даних, які потрібно класифікувати. Особливий інтерес також представляє вплив кодера на результати класифікації. Основні результати наступні. По-перше, точність класифікації майже однакова для класифікаторів, навчених для нестиснутих і змодельованих стиснутих даних для загальної моделі спотворення. По-друге, існує певна різниця в результатах класифікації для різних досліджуваних методів стиснення. Дещо кращі результати класифікації спостерігаються для даних, створених більш складними (сучасними) кодерами. Експерименти проведено на двох реальних триканальних зображеннях Харкова та Харківської області різної складності Sentinel-2. Розглянуто чотири типові класи. Як висновок, можна стверджувати, що або загальна модель спотворень повинна бути модифікована, або навчання класифікатора має бути виконано для даних, створених відповідною технікою стиснення.

Ключові слова: стиснення з втратами; триканальні зображення; класифікатор на основі нейронної мережі; навчальні дані.

Проскура Галина Анатоліївна – канд. техн. наук, доц. каф. інформаційно-комунікаційних технологій ім. О. О. Зеленського, Національний аерокосмічний університет ім. М. Є. Жуковського «Харківський авіаційний інститут», Харків, Україна.

Рубель Олексій Сергійович – канд. техн. наук, доцент кафедри інформаційно-комунікаційних технологій ім. О. О. Зеленського, Національний аерокосмічний університет ім. М. Є. Жуковського «Харківський авіаційний інститут», Харків, Україна.

Кривенко Сергій Станіславович – канд. техн. наук, старш. дослідник, старш. наук. співроб. каф. інформаційно-комунікаційних технологій ім. О. О. Зеленського, Національний аерокосмічний університет ім. М. Є. Жуковського «Харківський авіаційний інститут», Харків, Україна.

Лукін Володимир Васильович – д-р техн. наук, проф., зав. каф. інформаційно-комунікаційних технологій ім. О. О. Зеленського, Національний аерокосмічний університет ім. М. Є. Жуковського «Харківський авіаційний інститут», Харків, Україна.

Galina Proskura – Candidate of Technical Science, Associate Professor of Information-communication Technologies named after O. O. Zelensky Department, National Aerospace University “Kharkiv Aviation Institute”, Kharkiv, Ukraine,
e-mail: g.proskura@khai.edu, ORCID: 0000-0001-8960-0421.

Oleksiy Rubel – Candidate of Technical Science, Associate Professor of Information-communication Technologies named after O. O. Zelensky Department, National Aerospace University “Kharkiv Aviation Institute”, Kharkiv, Ukraine,
e-mail: o.rubel@khai.edu, ORCID: 0000-0001-6206-3988.

Sergii Kryvenko – Candidate of Technical Science, Senior Researcher of Information-communication Technologies named after O. O. Zelensky Department, National Aerospace University “Kharkiv Aviation Institute”, Kharkiv, Ukraine,
e-mail: krivenkosergiy@gmail.com, ORCID: 0000-0001-6027-5442.

Vladimir Lukin – Doctor of Technical Science, Professor, Head of Information-communication technologies named after O. O. Zelensky Department, National Aerospace University “Kharkiv Aviation Institute”, Kharkiv, Ukraine,
e-mail: lukin@ai.kharkov.com, ORCID: 0000-0002-1443-9685.